A&A, 686, A215 (2024)
https://doi.org/10.1051/0004-6361/202449393

Astronomy & Astrophysics

A fast-rotating blue straggler star in the tidal tail of the open cluster NGC 752

Chunyan Li (李春燕)[1,2], Jing Zhong (钟靖)[1], Songmei Qin (秦松梅)[1,2], Dengkai Jiang (姜登凯)[2,3,4], Xingmei Shan (单星美)[5], and Li Chen (陈力)[1,2]

[1] Key Laboratory for Research in Galaxies and Cosmology, Shanghai Astronomical Observatory, Chinese Academy of Sciences, 80 Nandan Road, Shanghai 200030, PR China
e-mail: lichunyan@shao.ac.cn;chenli@shao.ac.cn
[2] School of Astronomy and Space Science, University of Chinese Academy of Sciences, No. 19A, Yuquan Road, Beijing 100049, PR China
[3] Yunnan Observatories, Chinese Academy of Sciences, 396 Yangfangwang, Guandu District, Kunming 650216, PR China
[4] International Centre of Supernovae, Yunnan Key Laboratory, Kunming 650216, PR China
[5] Shanghai Science and Technology Museum, No. 2000 Century Avenue, Pudong New Area, Shanghai 200127, PR China

Received 30 January 2024 / Accepted 28 March 2024

ABSTRACT

Context. NGC 752 is a well-known Galactic open cluster of intermediate age. In recent works, a very long and asymmetric tail was revealed. A blue straggler star (BSS) at the periphery of the tidal tail of the cluster was subsequently identified.
Aims. We aim to perform a detailed analysis of the newly detected BSS based on the available comprehensive spectroscopic and photometric data. We also explored this BSS's possible formation pathway and age limitation based on the collected spectroscopic and photometric data.
Methods. We reconfirmed the membership of the newly determined BSS of NGC 752, supplemented by *Gaia* DR3 radial velocity data. Moreover, we also estimated the projected rotational velocity and the mass of the BSS from the Large Sky Area Multi-Object Fiber Spectroscopic Telescope low-resolution spectra and multiband photometric data from various catalogs, respectively.
Results. The newly discovered BSS is confirmed as a genuine member of NGC 752. The lack of ultraviolet excess in the spectral energy distribution and no significant variations in the light curve imply that this BSS is likely a single star (mass = $1.86^{+3.62}_{-0.94}\,M_{\odot}$) formed through stellar mergers. The fast rotation velocity ($v \sin i = 206.9 \pm 4.9\,\mathrm{km\,s^{-1}}$) of the BSS may provide constraints on its age (less than a hundred million years), but more formation details require further investigation.

Key words. blue stragglers – open clusters and associations: individual: NGC 752

1. Introduction

Blue straggler stars (BSSs) are typically characterized as a population of stars that are bluer and brighter than the main-sequence turn-off (MSTO) stars. They are observed as an extension of the main sequence positioned above the MSTO in the color-magnitude diagram (CMD). Hence, BSSs are thought to be more massive than MSTO stars (Shara et al. 1997; Gilliland et al. 1998; De Marco et al. 2005; Fiorentino et al. 2014), which implies that BSSs are the products of main-sequence stars that gained extra mass.

Blue straggler stars were first reported by Sandage (1953) in the CMD of the globular cluster M 3. In the Milky Way, BSSs are not only commonly identified in globular clusters (GCs; Piotto et al. 2004; Leigh et al. 2008) or dwarf spheroidal galaxies (Salinas et al. 2012), but they also exist in the intermediate-age or old open clusters (OCs; Ahumada & Lapasset 2007; Rain et al. 2021; Jadhav & Subramaniam 2021; Li et al. 2023).

There are multiple formation scenarios for creating BSSs: (i) direct stellar collisions during dynamical encounters (Hills & Day 1976; Leonard 1989); (ii) mass transfer from binary companions (McCrea 1964); (iii) mergers of two main sequence stars (Nelson & Eggleton 2001; Perets & Fabrycky 2009). Although the relationship between formation environment and the mechanism is still not completely understood (Leigh et al. 2007), collisional BSSs are more likely to be produced in the high-density environment and have been identified in a few GCs (Ferraro et al. 2009; Dalessandro et al. 2013; Beccari et al. 2019; Cadelano et al. 2022). However, BSSs formed from the evolution of binaries are also widely found in these GCs. Presently, the main leading BSS formation scenarios involve mass-transfer processes between binary companions, possibly up to the complete coalescence of the binary system, or mergers of stars induced by collisions (Ferraro et al. 2015). It is plausible that these formation mechanisms could be at work simultaneously in a given GC or OC. Andronov et al. (2006) quantified the angular momentum loss induced by magnetic stellar winds in tidally synchronized binaries on the main sequence and suggested that this mechanism is responsible for at least one-third of the BSSs in OCs older than 1 Gyr. It was also proposed in recent studies that BSS formed from the merger of main-sequence stars previously in a hierarchical triple system as a result of the eccentric Kozai–Lidov mechanism (Perets & Fabrycky 2009; Naoz & Fabrycky 2014), which has a significant role in BSS formation in OCs. Indeed, plenty of evidence supports the notion that multiple formation scenarios contribute to creating BSSs in open clusters (Jadhav & Subramaniam 2021; Leiner & Geller 2021).

NGC 752 is an open cluster with intermediate age of 1−1.5 Gyr (Agüeros et al. 2018; Cantat-Gaudin et al. 2020; Boffin et al. 2022). After comparing the initial mass and the present-day mass of NGC 752, we find that this cluster is experiencing a disintegration process since it has lost nearly 95.2%−98.5% of its initial mass due to stellar evolution and tidal interactions Bhattacharya et al. (2021). NGC 752 is centered at (l = 136.959°, b = −23.289°) and located about 483 pc away from the Sun, exhibiting a very small extinction (Cantat-Gaudin et al. 2020; Dias et al. 2021). In the earlier works, the cluster radius of the cluster is estimated as 84 arcmin (Kharchenko et al. 2013), and the mean half number radius is about 28.2 arcmin (Cantat-Gaudin & Anders 2020; Cantat-Gaudin et al. 2020; Dias et al. 2021).

However, with the help of *Gaia* data (Gaia Collaboration 2018, 2021), more and more studies have revealed the existence of outer halo region or extended tidal tails (Zhong et al. 2019, 2022; Zhang et al. 2020; Bai et al. 2022; Pang et al. 2022), leading to a significant increase in the size of OCs. Using *Gaia* EDR3 data (Gaia Collaboration 2021), Bhattacharya et al. (2021) extended the searching area for cluster member stars to a 5° radius around the center of NGC 752 and identified its tidal tails spanning up to 35 pc on both sides of the cluster center. Furthermore, Boffin et al. (2022) investigated a much wider region around NGC 752 and revisited its tidal tails. We find that the tidal tails of NGC 752 are considerably longer than what was previously claimed in Bhattacharya et al. (2021) and span over 260 pc in the sky (equivalent to 37° at the distance of NGC 752).

NGC 752 was first reported to host a BSS in the central area by Daniel et al. (1994). However, this BSS (hereafter named BS_D94) was absent from the BSS catalog of Ahumada & Lapasset (2007), which was referred to as the comprehensive catalog of BSSs in the Galactic open clusters up to 2005. This inconsistency may be attributed to different cluster membership determination results by various works, leading to different authentication results for BSS. In the *Gaia* era, Rain et al. (2021) identified 897 BSSs in 111 OCs using cluster member stars provided by Cantat-Gaudin & Anders (2020). Similarly, Jadhav & Subramaniam (2021) produced a catalog of 868 BSSs in 228 OCs with the membership information from Cantat-Gaudin et al. (2020). The two catalogs can be considered as an update to the catalog of Ahumada & Lapasset (2007). However, the BS_D94 was not included in either catalog because it was not regarded as a member star of NGC 752 by Cantat-Gaudin & Anders (2020), Cantat-Gaudin et al. (2020).

To identify more BSSs in a larger OC region, Li et al. (2023) extended the searching area and re-performed the membership determination of OCs, which was accomplished based on astrometric data from *Gaia* DR3 (Gaia Collaboration 2023) by the pyUPMASK[1] algorithm (Krone-Martins & Moitinho 2014; Pera et al. 2021). Finally, Li et al. (2023) identified 138 new BSSs in 50 open clusters, including a BSS (hereafter BS_Li23) in NGC 752. In particular, the BS_Li23 was discovered at the far end of the tidal tail with an angular distance extending over 8° from the center of NGC 752.

According to the results of Li et al. (2023), we found that approximately 91% of BSSs are distributed within three times half number radius (R_h) of their host OCs. However, the location of BS_Li23 in NGC 752 exceeds three times R_h, which may indicate that the formation process of BS_Li23 differs from most BSSs. We thus conducted a detailed analysis of the observational properties of BS_Li23 and further probed the possible formation way of BSSs in a low-density environment of open clusters.

In this work, we collected the optical spectroscopy, multi-band photometry, and time-domain photometry observational information, and then performed a detailed analysis of the BSS in NGC 752 reported by Li et al. (2023). In Sect. 2, we analyze the available spectroscopic and photometric data of BS_Li23 and extract properties of this BSS. We discuss the probable formation pathway and the age limitation of the BSS in Sect. 3. In Sect. 4, we reevaluate the membership of BS_D94 based on *Gaia* DR3 data. Finally, we give a summary in Sect. 5.

2. Properties of the BS_Li23

In this study, all members of NGC 752 are from the catalog of Li et al. (2023). In total, 404 member stars with membership probabilities (P_m) no less than 0.9 were identified in NGC 752 by Li et al. (2023), and these stars are regarded as NGC 752 member samples in this work. Considering that the differential reddening may introduce some dispersion on the CMD, especially near MSTO, which can affect the selection of BSS, we performed differential reddening (DR) correction on the CMD of NGC 752 referring to the method of Milone et al. (2012). As shown in Fig. 1, the DR-corrected CMD of NGC 752 presents a clear main sequence and an MSTO region, while a member star is located within the region delimited by the best-fitting isochrone and zero-age main sequence (ZAMS). We regarded this member star as a genuine BSS since it is located in the definition region of the typical BSSs in the CMD (Ahumada & Lapasset 1995, 2007; Rain et al. 2021). In this work, we named this BSS identified in NGC 752 as BS_Li23.

It is worth noting that in Fig. 1 there is a star at the reddest level of MSTO and fainter than the base of the sub-giant branch, marked as a filled square. From its unique location on the CMD, this star might be a potential sub-subgiant star (SSG). In the CMDs of star clusters, SSGs reside in the red of the main sequence, but they are fainter than the subgiant branch and are also known as red stragglers (Belloni et al. 1998; Mathieu et al. 2003). The origins of SSGs are not completely understood, as they are situated far from the predicted locus of single stars based on stellar evolution theory (Geller et al. 2015, 2017a,b; Leiner et al. 2017). This star may be the first identified SSG in NGC 752, and further detailed investigations on its characteristics and formation pathway would be of great value in future work.

2.1. Fundamental parameters

As shown in panel a of Fig. 2, BS_Li23 is situated about 8.3° away from the cluster center (RA = 29.404°, Dec = 37.7569°); nevertheless, the proper motion and parallax parameters of BS_Li23 are in accordance with other genuine NGC 752 member stars, as can be seen in panels b and c of Fig. 2.

The fundamental parameters for BS_Li23 provided by *Gaia* DR3 are listed in Table 1. We also presented the radial velocity (RV) distribution of NGC 752 member stars in panel d of Fig. 2. As reported in Katz et al. (2023), at G_{RVS} = 12 mag, the median formal precision of radial velocities can reach 1.3 km s^{-1}, and the exclusion of sources with low signal-to-noise ratio (S/N) spectra (S/N less than 10) effectively eliminates a notable proportion of outliers. We employed member stars with $G_{RVS} \leq 12$, $S/N > 10$ to estimate the average RV of NGC 752. After further removing four outliers, 45 main sequence stars are retained as a golden

[1] A python version of the Unsupervised Photometric Membership Assignment in Stellar Clusters algorithm (UPMASK).

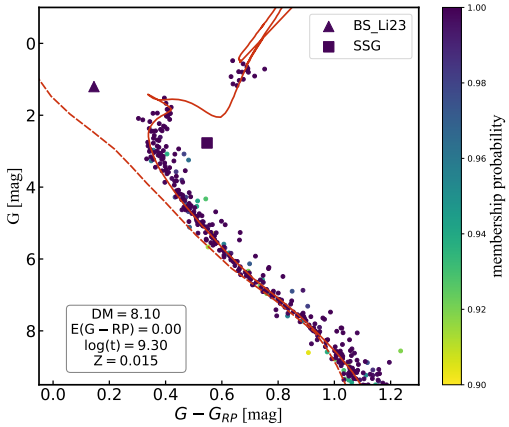

Fig. 1. Differential reddening corrected CMD of NGC 752. The triangle and square symbols represent the BSS of NGC 752 reported by Li et al. (2023) and an SSG candidate, respectively, while the dots denote cluster member stars. The solid red line represents the best-fitting isochrone, with parameters provided by Li et al. (2023). The red dashed line corresponds to the ZAMS. The color bar indicates the membership probability.

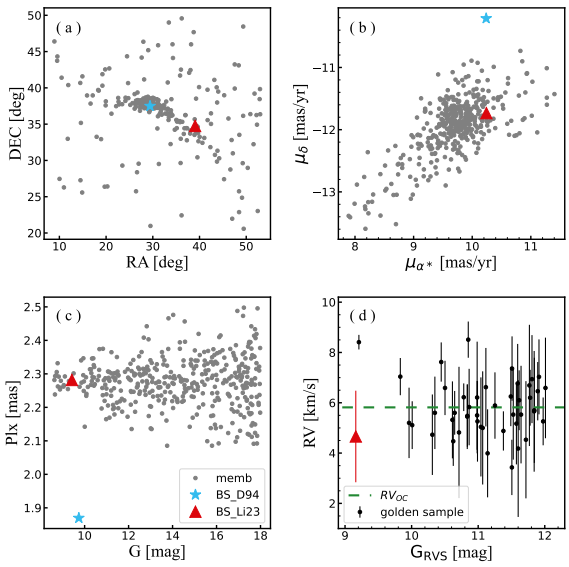

Fig. 2. Spatial distribution, proper motion distribution, magnitude-parallax diagram, and radial velocity distribution of NGC 752 member stars identified in Li et al. (2023) and a BSS reported by Daniel et al. (1994). Panels a–c: gray dots represent the cluster members of NGC 752 with $P_m \geq 0.9$; for comparison, the star categorized as a BSS of NGC 752 by Daniel et al. (1994) is symbolized by a blue pentagram, labeled BS_D94. Panel d: black dots represent member stars meeting the criteria of the golden sample described in Sect. 2.1; the RV and corresponding error is from *Gaia* DR3; the green dashed line presents the mean RV value of the golden sample. The BSS reported by Li et al. (2023) is marked as a red triangle labeled BS_Li23 in all panels.

sample, and the mean RV of these stars is 5.81 km s^{-1}, with the velocity dispersion of 1.06 km s^{-1}.

Moreover, there are 18 golden sample stars included in the Large Sky Area Multi-Object Fiber Spectroscopic Telescope (LAMOST) Medium-Resolution Spectroscopic (MRS) Survey Parameter Catalog[2]. The LAMOST, also named the *Guo Shou Jing* Telescope, is a four-meter quasi-meridian reflective Schmidt telescope with 4000 fibers (Cui et al. 2012), which was equipped with a medium-resolution spectrograph ($R \sim 7500$) with two arms covering the wavelength ranges of 495−535 nm and 630−680 nm, respectively (Liu et al. 2020). The average RV precision obtained from LAMOST MRS spectra reaches 1.0 km s^{-1} (Liu et al. 2019; Zong et al. 2020). The mean LAMOST RV of NGC 752 is 6.17 km s^{-1}, with a dispersion of 1.35 km s^{-1}, which is similar to the result of *Gaia* RV.

We notice that the *Gaia* DR3 radial velocity of BS_Li23 is 4.66 ± 1.82 km s^{-1}, showing good consistency with the radial velocity characteristic of NGC 752. Supplemented by *Gaia* DR3 radial velocity data, we thus re-confirmed that BS_Li23 is a genuine member BSS of NGC 752.

Table 1. Parameters of BS_Li23.

Parameter	Unit	Value	Source
RA (J2016)	deg	39.0595	*Gaia* DR3
Dec (J2016)	deg	34.7482	*Gaia* DR3
μ_{α^*}	mas yr^{-1}	10.24 ± 0.03	*Gaia* DR3
μ_δ	mas yr^{-1}	−11.73 ± 0.02	*Gaia* DR3
Plx	mas	2.28 ± 0.02	*Gaia* DR3
RV	km s^{-1}	4.66 ± 1.82	*Gaia* DR3
$v \sin i_{\rm esphs}$	km s^{-1}	179.18 ± 3.71	*Gaia* DR3
G	mag	9.422	*Gaia* DR3
$G_{\rm RVS}$	mag	9.162 ± 0.005	*Gaia* DR3
$T_{\rm eff}$	K	8310 ± 39	LAMOST DR9
log (g)	dex	3.96 ± 0.05	LAMOST DR9
[Fe/H]	dex	−0.095 ± 0.033	LAMOST DR9
$v \sin i_{\rm H\alpha}$	km s^{-1}	$210.3^{+2.5}_{-2.6}$	This work
$v \sin i_{\rm H\beta}$	km s^{-1}	$200.0^{+3.0}_{-2.6}$	This work
$v \sin i_{\rm H\gamma}$	km s^{-1}	$210.5^{+1.5}_{-2.5}$	This work
Mass	$M_\odot$	$1.86^{+3.62}_{-0.94}$	This work

2.2. Rotational velocity

The projected rotational velocity ($v \sin i$) of BS_Li23 is provided by the Extended Stellar Parameterizer for Hot Stars (ESP-HS) of *Gaia* DR3, and its value is listed in Table 1. However, considering the limitation of the spectra wavelength (845−872 nm), ESP-HS values suffer from the poor $v \sin i$-related information for OBA stars in this wavelength domain (Fouesneau et al. 2023). Besides *Gaia* DR3 data, the only spectrum data we can find for BS_Li23 is from the low-resolution spectra (LRS) of LAMOST Data Release 9 (DR9), whose designation name is J023614.26+344453.6, with an S/N of 60 at the effective wavelengths of the Sloan DSS g filter (Fukugita et al. 1996; Tucker et al. 2006). The wavelength range of the low-resolution spectra spans from 370 to 900 nm, and the spectral resolution is 1800 (Zhao et al. 2012). The LAMOST spectrum of BS_Li23, as shown in the top panel of Fig. 3, indicates it is an A-type star. The basic stellar parameters of BS_Li23 are provided in the LAMOST LRS Stellar Parameter Catalog of A, F, G, and K Stars[3]. In the catalog, the stellar spectral type of BS_Li23 is classed as A5, and the atmosphere parameters of the BS are $T_{\rm eff} = 8310 \pm 39$ K, log (g) = 3.96 ± 0.05, and [Fe/H] = −0.095 ± 0.033, which were determined by the LAMOST stellar parameter pipeline (LASP). However, this catalog does not provide the $v \sin i$ of stars.

To estimate the $v \sin i$ of BS_Li23 with the LAMOST data, we employed the χ^2 minimization method by comparing the

[2] http://www.lamost.org/dr10/v1.0/catalogue

[3] http://www.lamost.org/dr9/v2.0/catalogue

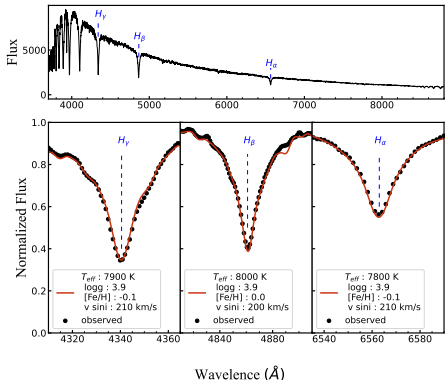

Fig. 3. Low-resolution LAMOST spectrum of BS_Li23 and best-fitting synthetic spectra for Balmer absorption lines. Top panel: low-resolution LAMOST spectrum of BS_Li23, showing the Balmer absorption lines. Bottom panel: Hγ, Hβ, and Hα lines along with their best-fitting models (red solid lines). The best-fitting parameters are shown in each panel.

observed LAMOST LRS to a grid of synthetic spectra for different values of $v \sin i$. Considering the spectral resolution ($R \sim 1800$) of LAMOST spectrum is low and the spectral type of BS_Li23 is A type, we chose to use the Balmer lines (Hα, Hβ, and Hγ) rather than other weak metal lines to determine the $v \sin i$ parameter. These high-resolution synthetic spectra were generated using the iSpec code (Blanco-Cuaresma et al. 2014; Blanco-Cuaresma 2019), an open-source framework for spectral analysis that integrates ATLAS9 model atmospheres (Kurucz 2005) with the radial transfer codes SYNTHE (Kurucz 1993; Sbordone et al. 2004). Referring to the parameters from the LAMOST DR9 catalog (listed in Table 1) for BS_Li23, the synthetic spectra were derived with $T_{\rm eff}$ range from 7500 K to 9500 K (in steps of 100 K), $\log(g)$ from 3.9 dex to 4.0 dex (in steps of 0.1 dex), and [Fe/H] from −0.2 dex to 0.2 dex (in steps of 0.1 dex). The microturbulence velocities of main-sequence early-type stars were about 0−3 km s^{-1} in previous works (Leckrone 1971; Mihalas 1972, 1973; Mucciarelli 2011). Hence, we assumed a microturbulent velocity of 2 km s^{-1} for BS_Li23 when generating the synthetic spectra. All the synthetic spectra were downgraded to the resolution from 80 000 to 1800 to match the LAMOST low-resolution spectra. Then, we convolved the synthetic spectra with different rotational kernels (Gray 2005) from $v \sin i = 5$ km s^{-1} to 300 km s^{-1} (in steps of 2 km s^{-1}). We further used a Monte Carlo method (Foreman-Mackey et al. 2013) to estimate the uncertainty in $v \sin i$ around the grid values. Finally, the synthetic spectra that minimized the χ^2 are shown in the bottom panel of Fig. 3, along with the parameters of these synthetic spectra and corresponding best-matched $v \sin i$. The estimated values of $v \sin i$ from the fitting results of Hα, Hβ, and Hγ lines are similar ($v \sin i_{\rm H\alpha} = 210.3^{+2.5}_{-2.6}$ km s^{-1}, $v \sin i_{\rm H\beta} = 200.0^{+3.0}_{-2.6}$ km s^{-1}, $v \sin i_{\rm H\gamma} = 210.5^{+1.5}_{-2.5}$ km s^{-1}). The average value of $v \sin i$ obtained from the results of the three lines is about 206.9 ± 4.9 km s^{-1}.

Frasca et al. (2016) mentioned that the $v \sin i$ determined from LAMOST LRS spectra can be considered reliable if the value exceeds 120 km s^{-1}. As stated in a recent work by Zuo et al. (2024), the LAMOST $v \sin i$ measurement precision is mainly affected by the S/N of spectra. They calculated the $v \sin i$ precision for 80 108 stars with multiple LAMOST LRS observations and estimated that the intrinsic precision of $v \sin i$ is about 10 km s^{-1} with an $S/N > 50$. This precision is acceptable for BS_Li23 with a large value of $v \sin i$ over 200 km s^{-1}. Comparing our result with *Gaia* DR3 $v \sin i_{\rm esphs}$, the difference is about 30 km s^{-1}, corresponding to about a 15% relative deviation at the high $v \sin i$ of about 200 km s^{-1}. Since the $v \sin i$ parameter has not been provided in the LAMOST LRS Stellar Parameter Catalog, we lack information regarding the overall systematic differences between LAMOST and *Gaia* in $v \sin i$. On the other hand, Zuo et al. (2024) found that the $v \sin i$ they estimated from LAMOST LRS spectra generally agree with *Gaia* $v \sin i_{\rm esphs}$ with a scatter of 24.7 km s^{-1} for 7013 common stars, which is also compatible to the difference in our work. Therefore, we regard BS_Li23 as a genuine fast-rotating BSS, given that it is relatively rare for BSSs to rotate faster than 50 km s^{-1} in both GCs (Ferraro et al. 2023a; Billi et al. 2023) and OCs (Mathieu & Geller 2009; Brady et al. 2023).

2.3. Stellar mass

In our investigation of the blue straggler BS_Li23, we used spectral energy distribution (SED) fitting to constrain its stellar mass. The SED fitting was performed by a python package ARIADNE[4], which aims to use Bayesian model averaging to incorporate the information from as many as six distinct atmospheric model grids to arrive at accurate and precise stellar parameters (Vines & Jenkins 2022). We collected multiband photometric data from various catalogs to fit the SED, including GALEX (FUV), *Tycho* (B and V), *Gaia* DR3 (G, $G_{\rm BP}$, and $G_{\rm RP}$), TESS (T), 2MASS (J, H, and K_s), and WISE ($W1$ and $W2$). We cross-matched BS_Li23 with other UV photometric catalogs, but only obtained FUV-band data from GALEX, which has been utilized in our SED fitting. Then, we used the atmospheric parameters from LAMOST DR9, parallax from *Gaia* DR3, and an extinction value of $A_v = 0$ obtained from Li et al. (2023) isochrone fitting result as prior parameters for the SED fitting. Figure 4 shows the SED fitting result. A single-star model can accurately represent the SED of BS_Li23. The best-fitting parameters with their 68% confidence intervals are as follows: $T_{\rm eff} = 8068^{+48.49}_{-83.55}$, $\log(g) = 4.05^{+0.23}_{-0.26}$, and $R = 2.718^{+0.033}_{-0.038}\,R_\odot$. We then calculated the stellar mass of BS_Li23 as $1.86^{+3.62}_{-0.94}\,M_\odot$ based on the derived stellar gravity and radius.

To explore the possible binarity property of BS_Li23, we first checked the variability flag of this star in *Gaia* DR3, but the flag of PHOT_VARIABLE_FLAG is marked as NOT_AVAILABLE for this star. Then, we analyzed the light curve from TESS (Ricker et al. 2015), which has been collected by TESS sectors 18 and 58. The light curve for this star, processed by the TESS Science Processing Operations Center (SPOC, Jenkins et al. 2016), is available on the *Mikulski* Archive for Space Telescopes (MAST) website[5] and shown in the top panel of Fig. 5. The PDCSAP_FLUX light curve is a detrended flux time series and also corrects for the amount of flux captured by the photometric aperture and crowding from known nearby stars. Then, we performed the Lomb-Scargle algorithm (Lomb 1976; Scargle 1982) to identify the potential period of the PDCSAP_FLUX light curve. The middle panel of Fig. 5 shows the Lomb-Scargle Periodogram, revealing a dominant frequency of approximately 0.223 day^{-1}. In the bottom panel of Fig. 5, the light curve in the top panel is folded at this period. However, hardly any variations in the phase-folded light curve of BS_Li23 could be detected. Therefore, BS_Li23 is unlikely to be a binary.

[4] https://github.com/jvines/astroARIADNE
[5] https://archive.stsci.edu/missions-and-data/tess

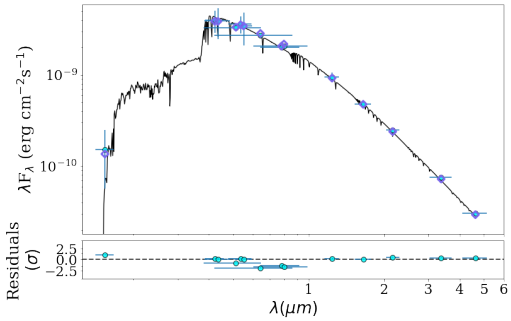

Fig. 4. Best-fitting SED model for BS_Li23. The black curve represents the best-fitting model, while the cyan pluses and circles denote the retrieved photometric measurements. The blue diamonds correspond to synthetic photometry.

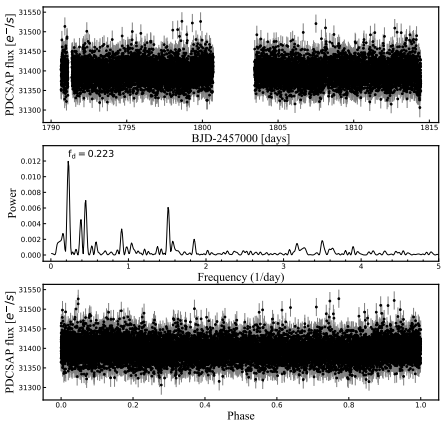

Fig. 5. TESS light curves for BS_Li23. Top panel: TESS pre-search data conditioning corrected simple aperture photometry (PDCSAP) light curve. Middle panel: Lomb-Scargle results for BS_Li23. Bottom panel: folded PDCSAP light curve at the dominant period.

3. Possible formation pathways and age limitation of BS_Li23

Several mechanisms are proposed for the formation of BSSs. Three major formation pathways of BSSs include (i) collisions during stellar dynamical encounters (Leonard 1989); (ii) mass transfer from a binary companion (McCrea 1964); (iii) mergers of close binary systems, perhaps the inner binaries in triple star systems driven to a merger by Kozai cycles (Perets & Fabrycky 2009).

Star collisions are generally believed to produce BSS, which is more common in environments with high stellar density, such as globular clusters. Compared to globular clusters, the density of open clusters is much lower, and the simulation indicates that the probability of producing BSSs through collisions in open clusters is very low (Geller et al. 2013). Furthermore, considering that BS_Li23 is located on the tidal tail of the disintegrating open cluster NGC 752 (Bhattacharya et al. 2021), its surrounding stellar density is much lower than the average cluster density. Therefore, the probability of this star being produced due to stellar collisions could be ignored.

Most BSSs are believed to have formed in open clusters through binary evolution (Mathieu & Geller 2015). This mechanism will generate a BSS + white dwarf (WD) system or a single BSS. The existence of a WD companion can be verified by examining whether there is an ultraviolet excess on the SED or flux variation in the light curve. As shown in Figs. 4 and 5, no ultraviolet excess appears on the SED of BS_Li23 (the ultraviolet data come from the FUV band of GALEX), and no observable significant optical variation signals can be detected from the light curve of BS_Li23, respectively. Meanwhile, the PHOT_VARIABLE_FLAG of this star is NOT_AVAILABLE in *Gaia* DR3. Based on existing results, we believe that BS_Li23 has a high probability of being a BSS single star produced by binary mergers.

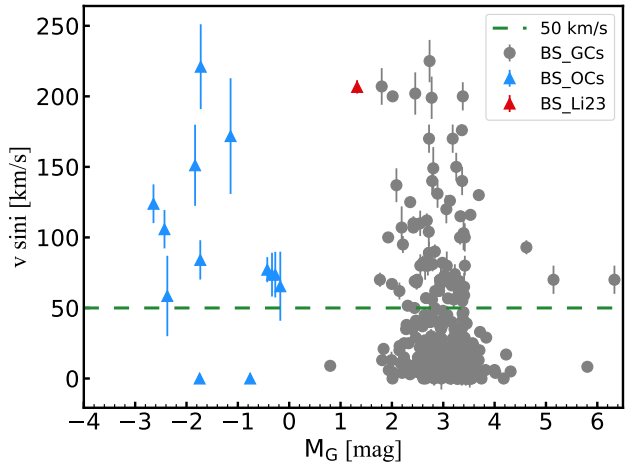

Fig. 6. Rotational velocity distributions as a function of absolute G magnitude. The BSSs in OCs reported by Li et al. (2023) are plotted as triangles, while BS_Li23 is marked as a red triangle. BSSs in GCs from Ferraro et al. (2023a) are denoted by gray dots. The $v \sin i$ errors for blue triangles, red triangles, and gray dots are from *Gaia* DR3, Sect. 2.2 of this work, and Ferraro et al. (2023a), respectively. Distance module and reddening for BSSs in GCs are all from the website (`https://people.smp.uq.edu.au/HolgerBaumgardt/globular`), while those for BSSs in OCs are from Li et al. (2023).

In the theoretical hypothesis of mass transfer in binary stars to form BSS, the orbital angular momentum of binary stars is accompanied by material transferred to the BSS, resulting in the newly formed BSS having a higher rotational speed (Sills et al. 2002; de Mink et al. 2013; Matrozis et al. 2017). Subsequently, due to the influence of the magnetic field, the BSS undergoes spin-down. Regarding observations, Ferraro et al. (2023a) confirmed 91 (about 28%) fast-rotating BSSs through high-resolution spectral observations of 320 BSSs. Furthermore, Leiner et al. (2018) studied the relationship between the BSS rotational velocity and age in open clusters. They also proposed that the BSS rotation begins to slow down on several hundred million year timescales, with a spin-down timescale of approximately 1−2 Gyr.

Based on the spectral fitting results of LAMOST, the $v \sin i$ of BS_Li23 is 206.9 ± 4.9 km s^{-1}. We then compared BS_Li23 with the 320 BSSs in GCs (Ferraro et al. 2023a) and 13 BSSs in OCs (Li et al. 2023). As shown in Fig. 6, it can be seen that BS_Li23 exhibits a characteristic of higher $v \sin i$ than most BSSs in both globular and open clusters observed so far, which implies that BS_Li23 may not have spun down yet. The rapid rotational velocity of a BSS may indicate its recent formation (Leiner et al. 2019). Based on the rough gyro-age relationship in Leiner et al. (2018), we expect the age of BS_Li23 to be restricted within a few hundred million years. Incidentally, NGC 752, the host open cluster of BS_Li23, is almost the oldest one among these OCs. Therefore, BS_Li23 appears to be more similar to the absolute magnitude of BSSs in globular clusters.

4. Reevaluation of a formerly labeled BSS

Before *Gaia* era, the comprehensive member catalogs of NGC 752 were from Daniel et al. (1994), Mermilliod et al. (1998), and Agüeros et al. (2018), while the determination of stellar members of NGC 752 was mainly based on ground observed proper motions and/or radial velocities. In Daniel et al. (1994), a star (BS_D94, *Gaia* DR3 source ID 342856660737416320) was identified as a probable member and located within the defined region of BSSs in the CMD (see Fig. 3 in Daniel et al. 1994). This star had retained as a cluster member of NGC 752 in subsequent studies (Mermilliod et al. 1998; Agüeros et al. 2018). Until the *Gaia* mission provided more precise astrometric data, BS_D94 was excluded from the members of NGC 752 in most updated OC catalogs (Cantat-Gaudin & Anders 2020; Cantat-Gaudin et al. 2020; Dias et al. 2021).

BS_D94 was not included by Li et al. (2023) in the initial sample for cluster membership determination. To investigate whether the star is a cluster member of NGC 752, we compared the characteristics of BS_D94 with that of cluster members ($P_{\rm m} \geq 0.9$) identified by Li et al. (2023). In Fig. 2, the proper motion and parallax of BS_D94 are considerably different from those high-probability member stars. The radial velocity of BS_D94 from *Gaia* DR3 is $-3.81\,{\rm km\,s^{-1}}$, which also significantly deviates from the average radial velocity value of NGC 752. We suggest that BS_D94 is likely a background field star that only happened to project near the cluster's center.

5. Summary

In the census work of BSSs by Li et al. (2023), a cluster member in the open cluster NGC 752 tidal tails was identified and classified as a BSS. We named this star BS_Li23 in this work and performed a detailed investigation.

We systematically collected and analyzed all available spectral and photometric data of BS_Li23. Firstly, the $v \sin i$ of BS_Li23 was derived as $206.9\,{\rm km\,s^{-1}}$ based on a LAMOST DR9 low-resolution spectrum, with a measurement precision level of about $10\,{\rm km\,s^{-1}}$. Subsequently, the mass of BS_Li23 was estimated by fitting its SED, combined from all available photometric datasets. The calculated mass of BS_Li23 is $1.859^{+3.62}_{-0.936}\,M_{\odot}$, which was derived from the best-fitting result of stellar gravity and radius. The SED of BS_Li23 can be appropriately represented by a single-star model, also compatible with the analysis of time series photometric data from TESS. Finally, we provided the fundamental parameters, estimated $v \sin i$, and stellar mass of BS_Li23 in Table 1.

Furthermore, we discussed the possible formation pathway and age of BS_Li23. Considering that this star is discovered in a low-density environment of tidal tail in the open cluster NGC 752, we believe that the stellar collision process could not practically be the formation pathway of this BSS. Because of the lack of FUV excess and flux variation, we speculate that this BSS was formed through binary evolution and has now merged into a single star. According to the formation theory of BSSs and the spin-down mechanism, the fast-rotating characteristic of BS_Li23 further demonstrates that it is a recently formed BSS.

It is worth noting that a star (BS_D94) was previously classified as a BSS in the literature. However, using the *Gaia* accurate astrometric data, we found that BS_D94 is significantly different in its kinematic and parallax parameters compared to high-probability member stars ($P_{\rm m} \geq 0.9$) identified by Li et al. (2023). We believe it is a background field star coincidentally projected into the central region of NGC 752.

In the *Gaia* era, our understanding of the spatial scale of open clusters has greatly expanded previous knowledge (Zhong et al. 2019; Meingast & Alves 2019; Bai et al. 2022). We now know that open clusters not only have high-density core components, but also low-density extended outer-halo components, which can even extend over a hundred pc (Zhong et al. 2022; Qin et al. 2023). Expanding the search region to hunt more BSSs in the open clusters is essential. Moreover, exploring the BSS in the external areas of OCs will provide new insights to investigate the different formation mechanisms of BSSs and the impact of varying cluster environments on BSS formation (Ferraro et al. 2012, 2023b).

Acknowledgements. We express our gratitude to the anonymous referee for their valuable comments and suggestions, which are very helpful in improving our manuscript. This work is supported by the National Natural Science Foundation of China (NSFC) through grants 12090040, 12090042, and 12073060. J.Z. would like to acknowledge the Youth Innovation Promotion Association CAS, the science research grants from the China Manned Space Project with NO. CMS-CSST-2021-A08, the Science and Technology Commission of Shanghai Municipality (Grant No. 22dz1202400). D.J. would like to acknowledge the National Key R&D Program of China No. 2021YFA1600403, the National Natural Science Foundation of China (Nos. 12073070, 12333008, 12288102, 12090040/3), International Centre of Supernovae, Yunnan Key Laboratory (No. 202302AN360001), Yunnan Revitalization Talent Support Program – Science & Technology Champion Project (No. 202305AB350003), the Yunnan Ten Thousand Talents Plan Young & Elite Talents Project, and Yunnan Fundamental Research Project (No. 202201BC070003, 202401BC070007). S.Q. acknowledges the financial support provided by the China Scholarship Council program(Grant No. 202304910547). This work has made use of data from the European Space Agency (ESA) mission *Gaia* (https://www.cosmos.esa.int/gaia), processed by the *Gaia* Data Processing and Analysis Consortium (DPAC, https://www.cosmos.esa.int/web/gaia/dpac/consortium). Funding for the DPAC has been provided by national institutions, in particular, the institutions participating in the *Gaia* Multilateral Agreement. Guoshoujing Telescope (the Large Sky Area Multi-Object Fiber Spectroscopic Telescope LAMOST) is a major national scientific Project built by the Chinese Academy of Sciences. Funding for the project has been provided by the National Development and Reform Commission. LAMOST is operated and managed by the National Astronomical Observatories, Chinese Academy of Sciences. This paper includes data collected with the TESS mission, obtained from the MAST data archive at the Space Telescope Science Institute (STScI). Funding for the TESS mission is provided by the NASA Explorer Program. STScI is operated by the Association of Universities for Research in Astronomy, Inc., under NASA contract NAS 526555.

References

Agüeros, M. A., Bowsher, E. C., Bochanski, J. J., et al. 2018, ApJ, 862, 33
Ahumada, J., & Lapasset, E. 1995, A&AS, 109, 375
Ahumada, J. A., & Lapasset, E. 2007, A&A, 463, 789
Andronov, N., Pinsonneault, M. H., & Terndrup, D. M. 2006, ApJ, 646, 1160
Bai, L., Zhong, J., Chen, L., Li, J., & Hou, J. 2022, Res. Astron. Astrophys., 22, 055022
Beccari, G., Ferraro, F. R., Dalessandro, E., et al. 2019, ApJ, 876, 87
Belloni, T., Verbunt, F., & Mathieu, R. D. 1998, A&A, 339, 431
Bhattacharya, S., Agarwal, M., Rao, K. K., & Vaidya, K. 2021, MNRAS, 505, 1607
Billi, A., Ferraro, F. R., Mucciarelli, A., et al. 2023, ApJ, 956, 124
Blanco-Cuaresma, S. 2019, MNRAS, 486, 2075
Blanco-Cuaresma, S., Soubiran, C., Heiter, U., & Jofré, P. 2014, A&A, 569, A111
Boffin, H. M. J., Jerabkova, T., Beccari, G., & Wang, L. 2022, MNRAS, 514, 3579
Brady, K. E., Sneden, C., Pilachowski, C. A., et al. 2023, AJ, 166, 154
Cadelano, M., Ferraro, F. R., Dalessandro, E., et al. 2022, ApJ, 941, 69
Cantat-Gaudin, T., & Anders, F. 2020, A&A, 633, A99
Cantat-Gaudin, T., Anders, F., Castro-Ginard, A., et al. 2020, A&A, 640, A1
Cui, X.-Q., Zhao, Y.-H., Chu, Y.-Q., et al. 2012, Res. Astron. Astrophys., 12, 1197
Dalessandro, E., Ferraro, F. R., Massari, D., et al. 2013, ApJ, 778, 135

Daniel, S. A., Latham, D. W., Mathieu, R. D., & Twarog, B. A. 1994, PASP, 106, 281
De Marco, O., Shara, M. M., Zurek, D., et al. 2005, ApJ, 632, 894
de Mink, S. E., Langer, N., Izzard, R. G., Sana, H., & de Koter, A. 2013, ApJ, 764, 166
Dias, W. S., Monteiro, H., Moitinho, A., et al. 2021, MNRAS, 504, 356
Ferraro, F. R., Beccari, G., Dalessandro, E., et al. 2009, Nature, 462, 1028
Ferraro, F. R., Lanzoni, B., Dalessandro, E., et al. 2012, Nature, 492, 393
Ferraro, F. R., Lanzoni, B., Dalessandro, E., Mucciarelli, A., & Lovisi, L. 2015, in Astrophysics and Space Science Library, eds. H. M. J. Boffin, G. Carraro, & G. Beccari, 413, 99
Ferraro, F. R., Mucciarelli, A., Lanzoni, B., et al. 2023a, Nat. Commun., 14, 2584
Ferraro, F. R., Lanzoni, B., Vesperini, E., et al. 2023b, ApJ, 950, 145
Fiorentino, G., Lanzoni, B., Dalessandro, E., et al. 2014, ApJ, 783, 34
Foreman-Mackey, D., Hogg, D. W., Lang, D., & Goodman, J. 2013, PASP, 125, 306
Fouesneau, M., Frémat, Y., Andrae, R., et al. 2023, A&A, 674, A28
Frasca, A., Molenda-Żakowicz, J., De Cat, P., et al. 2016, A&A, 594, A39
Fukugita, M., Ichikawa, T., Gunn, J. E., et al. 1996, AJ, 111, 1748
Gaia Collaboration (Brown, A. G. A., et al.) 2018, A&A, 616, A1
Gaia Collaboration (Brown, A. G. A., et al.) 2021, A&A, 649, A1
Gaia Collaboration (Vallenari, A., et al.) 2023, A&A, 674, A1
Geller, A. M., Hurley, J. R., & Mathieu, R. D. 2013, AJ, 145, 8
Geller, A. M., Latham, D. W., & Mathieu, R. D. 2015, AJ, 150, 97
Geller, A. M., Leiner, E. M., Bellini, A., et al. 2017a, ApJ, 840, 66
Geller, A. M., Leiner, E. M., Chatterjee, S., et al. 2017b, ApJ, 842, 1
Gilliland, R. L., Bono, G., Edmonds, P. D., et al. 1998, ApJ, 507, 818
Gray, D. F. 2005, The Observation and Analysis of Stellar Photospheres (Cambridge: Cambridge University Press)
Hills, J. G., & Day, C. A. 1976, Astrophys. Lett., 17, 87
Jadhav, V. V., & Subramaniam, A. 2021, MNRAS, 507, 1699
Jenkins, J. M., Twicken, J. D., McCauliff, S., et al. 2016, in Software and Cyberinfrastructure for Astronomy IV, eds. G. Chiozzi, & J. C. Guzman, SPIE Conf. Ser., 9913, 99133E
Katz, D., Sartoretti, P., Guerrier, A., et al. 2023, A&A, 674, A5
Kharchenko, N. V., Piskunov, A. E., Schilbach, E., Röser, S., & Scholz, R. D. 2013, A&A, 558, A53
Krone-Martins, A., & Moitinho, A. 2014, A&A, 561, A57
Kurucz, R. 1993, ATLAS9 Stellar Atmosphere Programs and 2 km/s Grid (Cambridge: Smithsonian Astrophysical Observatory)
Kurucz, R. L. 2005, Mem. Soc. Astron. It. Suppl., 8, 14
Leckrone, D. S. 1971, A&A, 11, 387
Leigh, N., Sills, A., & Knigge, C. 2007, ApJ, 661, 210
Leigh, N., Sills, A., & Knigge, C. 2008, ApJ, 678, 564
Leiner, E. M., & Geller, A. 2021, ApJ, 908, 229
Leiner, E., Mathieu, R. D., & Geller, A. M. 2017, ApJ, 840, 67
Leiner, E., Mathieu, R. D., Gosnell, N. M., & Sills, A. 2018, ApJ, 869, L29
Leiner, E., Mathieu, R. D., Vanderburg, A., Gosnell, N. M., & Smith, J. C. 2019, ApJ, 881, 47
Leonard, P. J. T. 1989, AJ, 98, 217
Li, C., Zhong, J., Qin, S., & Chen, L. 2023, A&A, 672, A81
Liu, N., Fu, J.-N., Zong, W., et al. 2019, Res. Astron. Astrophys., 19, 075
Liu, C., Fu, J., Shi, J., et al. 2020, arXiv e-prints [arXiv:2005.07210]
Lomb, N. R. 1976, Astrophys. Space Sci., 39, 447
Mathieu, R. D., & Geller, A. M. 2009, Nature, 462, 1032
Mathieu, R. D., & Geller, A. M. 2015, in Astrophysics and Space Science Library, eds. H. M. J. Boffin, G. Carraro, & G. Beccari, 413, 29
Mathieu, R. D., van den Berg, M., Torres, G., et al. 2003, AJ, 125, 246
Matrozis, E., Abate, C., & Stancliffe, R. J. 2017, A&A, 606, A137
McCrea, W. H. 1964, MNRAS, 128, 147
Meingast, S., & Alves, J. 2019, A&A, 621, L3
Mermilliod, J. C., Mathieu, R. D., Latham, D. W., & Mayor, M. 1998, A&A, 339, 423
Mihalas, D. 1972, ApJ, 177, 115
Mihalas, D. 1973, ApJ, 179, 209
Milone, A. P., Piotto, G., Bedin, L. R., et al. 2012, A&A, 540, A16
Mucciarelli, A. 2011, A&A, 528, A44
Naoz, S., & Fabrycky, D. C. 2014, ApJ, 793, 137
Nelson, C. A., & Eggleton, P. P. 2001, ApJ, 552, 664
Pang, X., Tang, S.-Y., Li, Y., et al. 2022, ApJ, 931, 156
Pera, M. S., Perren, G. I., Moitinho, A., Navone, H. D., & Vazquez, R. A. 2021, A&A, 650, A109
Perets, H. B., & Fabrycky, D. C. 2009, ApJ, 697, 1048
Piotto, G., De Angeli, F., King, I. R., et al. 2004, ApJ, 604, L109
Qin, S., Zhong, J., Tang, T., & Chen, L. 2023, ApJS, 265, 12
Rain, M. J., Ahumada, J. A., & Carraro, G. 2021, A&A, 650, A67
Ricker, G. R., Winn, J. N., Vanderspek, R., et al. 2015, J. Astron. Telesc. Instrum. Syst., 1, 014003
Salinas, R., Jílková, L., Carraro, G., Catelan, M., & Amigo, P. 2012, MNRAS, 421, 960
Sandage, A. R. 1953, AJ, 58, 61
Sbordone, L., Bonifacio, P., Castelli, F., & Kurucz, R. L. 2004, Mem. Soc. Astron. It. Suppl., 5, 93
Scargle, J. D. 1982, ApJ, 263, 835
Shara, M. M., Saffer, R. A., & Livio, M. 1997, ApJ, 489, L59
Sills, A., Adams, T., Davies, M. B., & Bate, M. R. 2002, MNRAS, 332, 49
Tucker, D. L., Kent, S., Richmond, M. W., et al. 2006, Astron. Nachr., 327, 821
Vines, J. I., & Jenkins, J. S. 2022, MNRAS, 513, 2719
Zhang, Y., Tang, S.-Y., Chen, W. P., Pang, X., & Liu, J. Z. 2020, ApJ, 889, 99
Zhao, G., Zhao, Y.-H., Chu, Y.-Q., Jing, Y.-P., & Deng, L.-C. 2012, Res. Astron. Astrophys., 12, 723
Zhong, J., Chen, L., Kouwenhoven, M. B. N., et al. 2019, A&A, 624, A34
Zhong, J., Chen, L., Jiang, Y., Qin, S., & Hou, J. 2022, AJ, 164, 54
Zong, W., Fu, J.-N., De Cat, P., et al. 2020, ApJS, 251, 15
Zuo, F., Luo, A. L., Du, B., et al. 2024, ApJS, 271, 4